Computer package for calculating electric and magnetic fields exploiting dual energy bounds

J.K. Sykulski, MSc, PhD, CEng, MIEE

Indexing terms: Electromagnetics, Magnetic fields, Mathematical techniques, Computer applications

Abstract: A computer graphics package, exploiting dual energy bounds for calculation of circuit parameters (R, L, C), has been recently developed in Southampton and implemented on a small desk-top computer. Simple pre- and postprocessing and considerable savings of computer time in comparison with other techniques are the most distinctive features of the method. The paper gives a brief description of this new software.

List of symbols

$\boldsymbol{A}$ = magnetic vector potential
$\boldsymbol{B}$ = magnetic flux density
C = capacitance
$\boldsymbol{D}$ = electric flux density
$\boldsymbol{E}$ = electric field strength
$\boldsymbol{H}$ = magnetic field strength
$\boldsymbol{I}$ = surface current (line density)
$\boldsymbol{J}$ = volume current (area density)
L = inductance
R = resistance
U = energy
ε = permittivity
μ = permeability
ρ = volume charge density
σ = area charge density
ϕ = electric scalar potential

1 Introduction

TAS (tubes and slices) is a suite of programs solving certain classes of problems which can be described by two-dimensional equations of the Laplacian or Poissonian types. A discretisation process involves splitting the system into a set of slices bounded by equipotential surfaces and into a set of tubes bounded by flux barriers. These two systems are then used to provide upper and lower bounds for the system energy. The technique is known as the method of tubes and slices, and this term will be used throughout the paper.

Owing to the relatively small amount of data needed for tubes and slices analysis and the method of solution, which avoids cumbersome matrix inversion, pre- and postprocessing is simple and solution times are extremely short. Dual bounds for values of circuit parameters are provided giving confidence limits for the solution and forming a criterion for interactive mesh adaptation.

The mathematical basis of the method, thorough discussion of its mathematical and physical implications and the state of the art in the development of the tubes and slices techniques may be found in the works by Hammond [1–3]. The emphasis of this paper is on computational aspects and computer-aided implementation of the method.

Paper 5870A (S8), first received 5th May and in revised form 25th November 1987

The author is with the Department of Electrical Engineering, The University, Southampton SO9 5NH, United Kingdom

2 Mathematical background

In magnetostatic fields the equilibrium conditions of the system can be described by two variational principles applied within the volume [1]:

$$\langle(\nabla \times \boldsymbol{H} - \bar{\boldsymbol{J}}), \delta\boldsymbol{A}\rangle = 0 \tag{1}$$

and

$$\langle(\nabla \times \boldsymbol{A} - \boldsymbol{B}), \delta\boldsymbol{H}\rangle = 0 \tag{2}$$

where the brackets $\langle\rangle$ indicate integration through the region of interest, and $\bar{\boldsymbol{J}}$ is the assigned current density.

The field energy can be expressed, either in terms of the field vectors $\boldsymbol{H}$ and $\boldsymbol{B}$:

$$U = \tfrac{1}{2}\langle\boldsymbol{B}, \boldsymbol{H}\rangle \tag{3}$$

or in terms of the interaction of the current sources with the vector potential $\boldsymbol{A}$:

$$U = \tfrac{1}{2}\langle\bar{\boldsymbol{J}}, \boldsymbol{A}\rangle + \tfrac{1}{2}[\bar{\boldsymbol{I}}, \boldsymbol{A}] \tag{4}$$

where $\bar{\boldsymbol{I}}$ is the assigned line density of current on the surface, and the brackets [] represent integration over the closed boundary surface.

The two variational principles can be applied to the whole system as [3]

$$\delta U(\boldsymbol{A}) = \delta\{-\tfrac{1}{2}\langle\boldsymbol{H}, \boldsymbol{B}\rangle + \langle\bar{\boldsymbol{J}}, \boldsymbol{A}\rangle + [\bar{\boldsymbol{I}}, \boldsymbol{A}]\} = 0 \tag{5}$$

where $\boldsymbol{H}$ and $\boldsymbol{B}$ are functions of $\boldsymbol{A}$, and

$$\delta U(\boldsymbol{H}) = \delta\{\tfrac{1}{2}\langle\boldsymbol{B}, \boldsymbol{H}\rangle\} = 0 \tag{6}$$

where $\boldsymbol{B}$ is a function of $\boldsymbol{H}$ through the constitutive field equation:

$$\boldsymbol{B} = \mu\boldsymbol{H} \tag{7}$$

For simplicity μ is assumed to be constant.

The second variations derived from eqns. 5 and 6 have different signs

$$\delta^2 U(\boldsymbol{A}) \leqslant 0 \tag{8}$$

and

$$\delta^2 U(\boldsymbol{H}) \geqslant 0 \tag{9}$$

so that the equilibrium energy is either a maximum (eqns. 5 and 8) or a minimum (eqns. 6 and 9).

The electrostatic field can be treated in an analogous manner [2]:

$$\delta U(\phi) = \delta\{\langle \bar{\rho}, \phi\rangle + [\bar{\sigma}, \phi] - \tfrac{1}{2}\langle \varepsilon | \nabla\phi|^2\rangle\} = 0 \quad (10)$$

$$\delta U(\boldsymbol{D}) = \delta\left\{\frac{1}{2}\left\langle \frac{1}{\varepsilon} | \boldsymbol{D}|^2 \right\rangle\right\} = 0 \quad (11)$$

$$\delta^2 U(\phi) \leqslant 0 \quad (12)$$

$$\delta^2 U(\boldsymbol{D}) \geqslant 0 \quad (13)$$

giving concave (eqns. 10 and 12) or convex (eqns. 11 and 13) energy functionals, respectively. Some other possibilities are also explored in Reference 2.

It will have been noticed that both variational principles of eqns. 1 and 2 lead to energy functionals, although one uses a variation in $\boldsymbol{A}$ and the other a variation in $\boldsymbol{H}$. The use of the vector potential in eqn. 1 gives the magnetic field as

$$\boldsymbol{B} = \nabla \times \boldsymbol{A} \quad (14)$$

which implies that the variation maintains the condition of zero volume divergence by enforcing $\nabla \cdot \boldsymbol{B} = 0$. Eqn. 2, on the other hand, uses the relationship

$$\nabla \times \boldsymbol{H} = \bar{\boldsymbol{J}} \quad (15)$$

and, as $\bar{\boldsymbol{J}}$ is fixed, this variation keeps the curl sources constant in the volume.

The two mechanisms are equivalent to introducing additional 'fictitious' sources inside the volume and on its boundary. Eqn. 5 introduces a fictitious volume current and surface current density, as well as a surface pole distribution. When both types of sources (curl and divergence) are varied, the system energy is decreased. Eqn. 6, on the other hand, introduces only divergence sources (fictitious pole density) and the energy is increased. All fictitious sources are zero at equilibrium and the whole process is controlled by the uniqueness of the field within the system [3].

Most of the popular methods like finite elements, boundary elements and finite differences ensure only that the total fictitious-source distribution of the whole system is zero. The use of free topology in such methods means also that information contained in boundary conditions is lost locally and a solution of simultaneous equations is required, which may be a very costly process. The accuracy that a particular discretisation will yield depends on the number of elements used, but is also a function of the experience of the user. Much benefit may be gained by applying dual and complementary methods to finite-element techniques to provide an absolute assessment of error in a given solution, and aid the generation of meshes. Some computer implementations of such schemes already exist (see, for example, References 4 or 5). An interesting dual finite-element formulation may be found in Reference 6. As expected, the computational effort can be considerably reduced in comparison with a standard finite-element method, but the solution of simultaneous equations still remains the crux of the approach. In seeking economies in the computation, the method of 'tubes and slices' goes one step further.

Introduction of tubes (bounded by flux barriers) and slices (bounded by equipotential surfaces) has many advantages. It treats the system as a whole and does not separate local conditions from the overall boundary conditions. On the contrary, it is now the boundary which governs the process of the solution. Secondly, the distribution of fictitious sources is under more strict control. The tubes introduce curl sources and the slices generate divergence sources, but the condition of zero total fictitious source distribution applies to individual slice or tube boundaries, not only to the whole system. Thirdly, and from the practical point of view, most importantly, the combined effect of this approach leads to very simple calculations completely avoiding the time-consuming matrix inversion.

3 Implementation of the method

In Laplacian fields, each slice carries the total flux and each tube has the same potential difference applied to its ends; therefore, calculations are reduced to summation of circuit parameters of all tubes or slices. For example, the resistance of a conductor of any shape, after a proper discretisation has been achieved, will be found as the series/parallel connection of a set of subconductors formed by the tube and slice subdivisions. All subconductors have a simple shape and the final explicit formulas for the resistance may be easily found. The slice system will produce the lower bound of the resistance, while the tube system gives the upper bound.

It will be noted that the division of the system into slices and tubes is physically well based, because it uses the potential and flux properties of the field.

In Poissonian fields we have to work in terms of the energy, instead of the circuit parameters of tubes and slices, to take account of the interaction due to distributed assigned volume sources. The lower and upper bounds of energy are then used to define the bounds of an overall circuit parameter, such as an inductance.

Implementation of the method of tubes and slices is very straightforward in principle. The troublesome solution stage has been eliminated and replaced by simple and fast calculation of the relevant circuit parameter. Emphasis is then directed to convenient and efficient ways of generating and improving the distribution of tubes and slices. Like any other numerical method the first solution does not guarantee a good answer. Unlike most other methods, however, dual bounds of the tubes and slices solution provide both confidence limits and a criterion for any further improvements. Another important difference is that it is the shape of both tubes and slices, not their number, which determines the accuracy of the method. The usual process of global or local mesh refinement is replaced by a procedure of reshaping the distribution of the two systems.

Special techniques must be used to handle material changes and interfaces or to deal with nonlinear systems. Some suggestions have been put forward in the References and such schemes will be incorporated into the TAS software, but are beyond the scope of this paper.

4 Discretisation

It is important to note that the two systems of tubes and slices may be treated completely independently of each other. It is only under equilibrium conditions that they become orthogonal, but such a perfect solution is rarely required. It is convenient, however, for the purpose of preprocessing to use the same mesh, or construction points, so as to generate both systems at the same time. After subsequent changes to the mesh and several calculations, a global minimum of all upper bound answers and a global maximum of all lower bound values are sought. These minimum and maximum values may and,

for most cases, will be different for different mesh configurations. At this point, the tubes and slices solutions are therefore separated.

It is also useful to notice that the method can use the same discretisation process for various fields under consideration. Hence, preprocessing can be a common step after which the appropriate formula will be chosen, depending on which circuit parameter is required.

A quadrilateral of general shape is chosen as a building block for constructing a mesh. This is a natural choice to match the inherent property of fields having two flux and two equipotential boundaries. The triangular element, so successful in finite elements, unfortunately completely destroys this symmetry. An interesting technique of a quadrilateral with an additional internal construction point is described in Reference 2. Although useful for hand calculations, this technique puts severe constraints on the freedom of defining other quadrilaterals to complete the system and would make any further movement of construction points very difficult.

The TAS program uses a quadrilateral with one diagonal, the direction of which may be chosen as illustrated in Fig. 1. A set of such quadrilaterals is used to match a

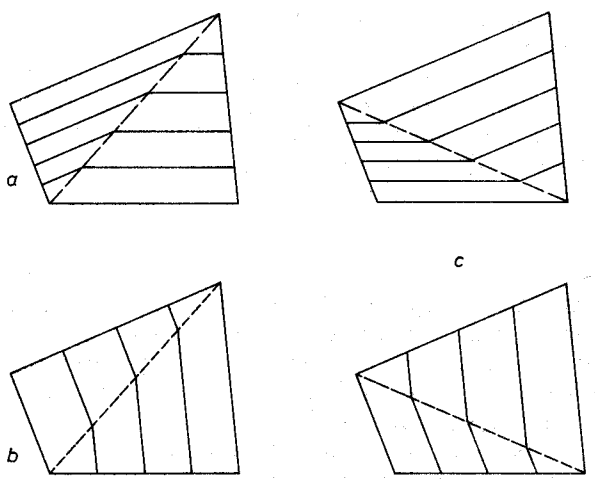

Fig. 1 *Subtubes (a) and subslices (b) in a quadrilateral, alternative system (c)*

particular shape of system boundaries. The distribution of both systems of tubes and slices is formed at the same time. Each tube and each slice may be further subdivided into subtubes and subslices to improve the accuracy of computation.

Once the two distributions have been set up, upper and lower bounds of a required system parameter (R, C or L) may be calculated. For R and C this process involves finding the total resistance (capacitance) of a system of series/parallel connections of resistances (capacitances) of all subtubes and subslices. Consider a system divided into t tubes and s slices. Each tube is split into m_i subtubes ($i = 1, \ldots, t$) and each slice has n_j subslices ($j = 1, \ldots, s$). In the TAS program these subdivisions are carried out automatically, but the process is controlled through specification of the number of subdivisions (values of m_i and n_j). As a simple illustration, let us consider the resistance of a conductor of Fig. 2*a*, for which we shall assume $t = 2$, $s = 3$ and $m_1 = m_2 = 6$, $n_1 = n_3 = 4$, $n_2 = 5$. The resultant distributions of all subtubes and subslices are shown in Fig. 2*b* and Fig. 2*c*, respectively. Each subtube consist of $2 \times s$ pieces of conductor connected in series and there are $M = \sum_i m_i$ subtubes in parallel. Similarly, each subslice is formed by $2 \times t$ pieces connected in parallel and $N = \sum_j n_j$ subslices are then connected in series. The formulas for the upper bound (tubes) and lower bound (slices) of the resistance are

$$R_+ = \frac{1}{\sum_{i=1}^{M} \left[1 \Big/ \left(\sum_{l=1}^{2s} r_{li} \right) \right]} \tag{16}$$

$$R_- = \sum_{j=1}^{N} \frac{1}{\sum_{k=1}^{2t} \frac{1}{r_{kj}}} \tag{17}$$

where r_{li} and r_{kj} denote the resistances of subconductors (per unit depth in 2-dimensional problems). Each subconductor has a simple shape and its resistance may be

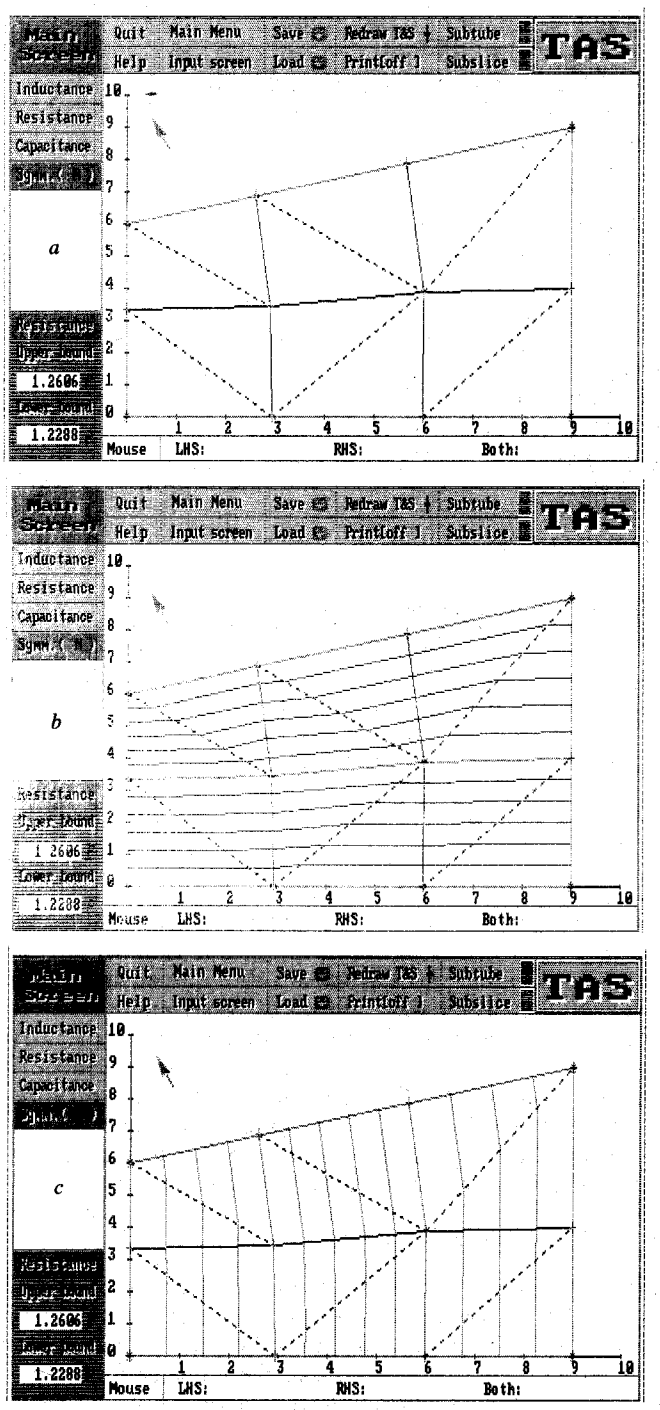

Fig. 2 *Calculation of resistance between a pair of vertical electrodes*

(*a*) System of construction lines defining a set of quadrilaterals giving two tubes and three slices
(*b*) Distribution of subtubes
(*c*) Distribution of subslices

approximated as

$$r_{li} = \frac{\text{mean length}}{\text{width}} \times \text{resistivity} \tag{18}$$

or

$$r_{kj} = \frac{\text{length}}{\text{mean width}} \times \text{resistivity} \tag{19}$$

An analogous argument holds for the capacitance of a system. Here the subdivision into tubes produces the lower bound, whereas slices give the upper bound of the capacitance. We have, therefore,

$$C_+ = \frac{1}{\sum_{j=1}^{N}\left[1\Big/\left(\sum_{k=1}^{2t} C_{kj}\right)\right]} \tag{20}$$

$$C_- = \sum_{i=1}^{M} \frac{1}{\sum_{l=1}^{2s} \frac{1}{C_{li}}} \tag{21}$$

where C_{kj} and C_{li} denote the capacitances of component pieces.

Calculation of an internal inductance involves working in terms of the energy instead of the circuit parameters, as already mentioned in Section 3. A possible approximation leads to the following formulas:

for tubes:

$$L_- = \frac{\mu_0}{S^2} \sum_{i=1}^{M} \frac{(\Delta S_i)^2}{\sum_{l=1}^{2s} \frac{l_{li}}{b_{li}}} \tag{22}$$

for slices:

$$L_+ = \frac{\mu_0}{S^2} \sum_{j=1}^{N} \sum_{k=1}^{2t} b_{jk}\left(\frac{l_{jk}^3}{3} + l_{jk}^2 H_{bjk} + l_{jk} H_{bjk}^2\right) \tag{23}$$

where S is the total area of the system, ΔS_i is the area below the centre line of the ith subtube, l_{li} and b_{li} are the length and width of an element of a subtube, l_{jk} and b_{jk} are the length and width of an element of a slice, H_{bjk} is the value of the field at the bottom of the kth piece of subslice j, and approximately

$$H_{t,j,k-1} b_{j,k-1} = H_{b,j,k} b_{j,k} \tag{24}$$

where $H_{t,j,k-1}$ is the magnetic field at the top of the $(k-1)$th section, while

$$H_{t,j,k} = l_{jk} + H_{bjk} \tag{25}$$

and the current density is assumed as constant throughout the region.

Details about the derivation of eqns. 22 and 23 may be found in Reference 3.

The simplicity of the final expressions (eqns. 16 to 25) is very striking and should be contrasted with the complexity of the normal finite-element formulation. Although the TAS method, like indeed most other methods, usually calls for more than one calculation to achieve the desired accuracy, this should hardly matter in view of this simplicity of computation.

5 The TAS software

The TAS program uses interactive graphics and full colour displays. It works in menu-driven mode and most operations are performed using a mouse. As the solution step involves only simple calculations, there are no special memory requirements and the only limitation is due to the graphic capabilities of a particular machine.

The structure of the TAS program is shown in Fig. 3. Extensive 'Help' facilities are provided throughout the

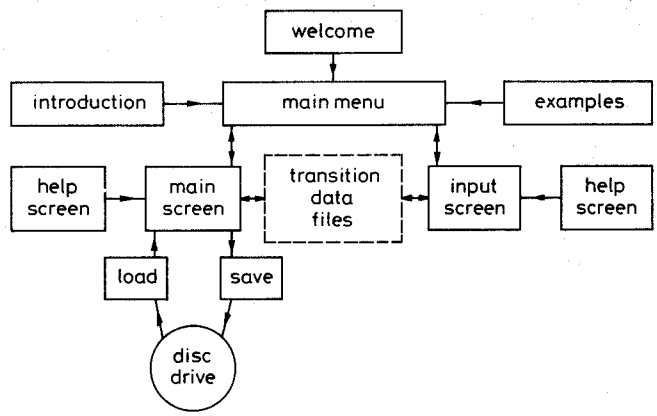

Fig. 3 *TAS program flowchart*

program. These include an introduction to the method and examples (called from the 'Main Menu') as well as a built-in manual in the form of two 'Help' programmes. Particular solutions may be stored on a disc using 'save' and 'load' options.

Two programs handle most of the important operations. The 'Input Screen' provides an interactive data input and mesh reshaping; the 'Main Screen' is used for obtaining a solution and for postviewing.

Setting up a problem for solution involves three steps. First, the geometric shape of the device to be described to the computer. Corner point locations are defined by entering their co-ordinates through the keyboard and the program responds by drawing the picture on the screen (see the example in Fig. 4). Next, the decision is made

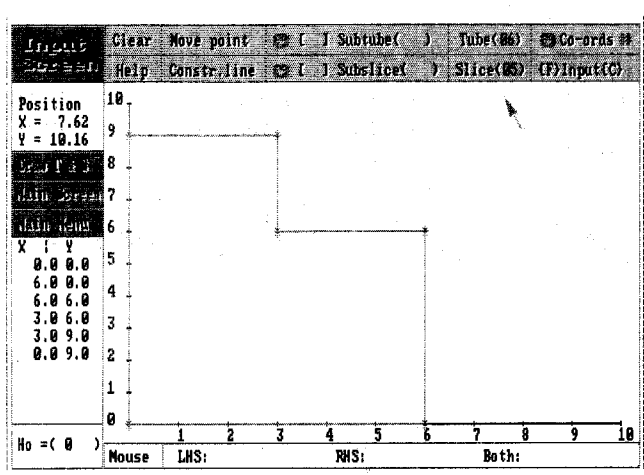

Fig. 4 *External boundary of the problem*

about the number of tubes t and slices s to be used for the solution, together with the information about additional subdivisions into subtubes and subslices (refer to the example in Section 4). Finally, $(t+1) \times (s+1)$ construction points are entered using a mouse. These construction points define corners of all fundamental quadrilaterals (as shown in Figs. 1 and 2*a*) and must be specified in a particular sequence along tube boundaries (see Figs. 5 and 6). To adjust the shape of tubes and slices two options are available: 'Move point' and 'Construction line'. Repositioning construction points is the main

tool for improving accuracy. Choosing a different direction of a diagonal construction line will also produce minor adjustments to the field shape, as shown in Fig. 1.

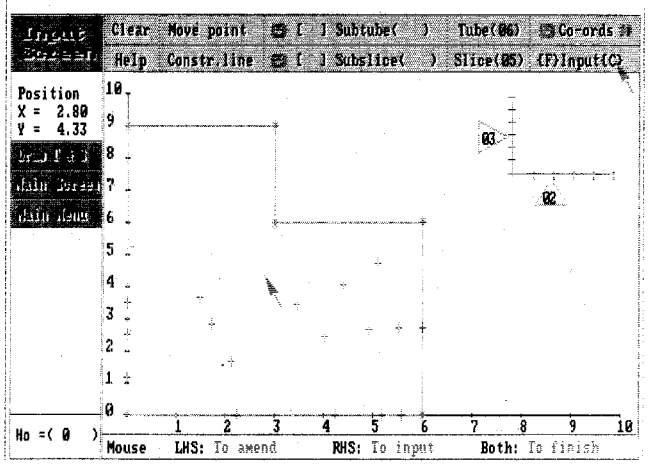

Fig. 5 *Entering the construction points*

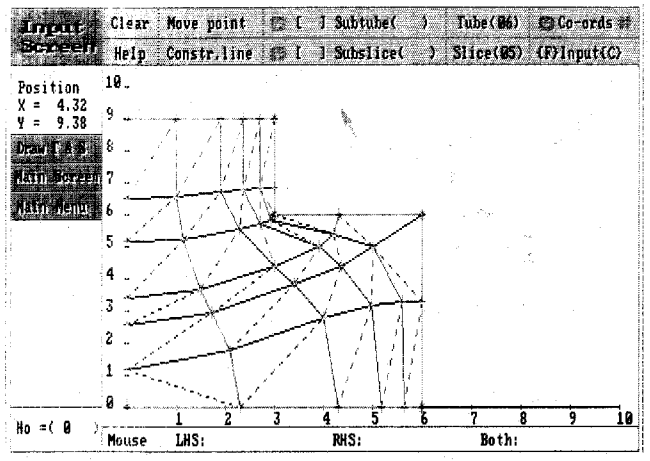

Fig. 6 *Distribution of construction lines*

The 'Main Screen' (Fig. 7) carries out calculations of dual bounds of circuit parameters (R, C or L), controls peripheral devices (disc drive, printer) and offers some simple postviewing facilities.

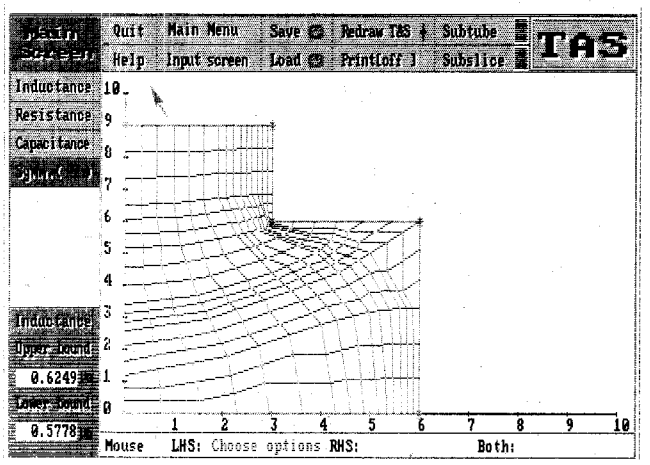

Fig. 7 *Calculation of internal inductance for the system of Fig. 6*

The dialogue between the 'Input Screen' and the 'Main Screen' may continue until a satisfactory solution has been obtained. It can be stressed again, however, that any change to the tube/slice distribution and the subsequent solution require very little computational effort.

6 Computing times and accuracy

As mentioned before, thanks to the simplicity of the computational scheme, the solution times are remarkably short: of the order of seconds on a personal computer. Implications of this fact cannot be overestimated. Combined with very modest requirements in terms of computer capabilities it furnishes a truly low-cost CAD facility. As an additional bonus, the provision of dual bounds on solutions gives stricter control over a CAD process.

No particular attention has to be paid initially to the shape of both systems of tubes and slices, as the average of the two bounds is likely to be within a few per cent of the correct answer, even if the values themselves are diverse. Both bounds can be improved at later stages to increase confidence in the solution, but insistence on having a perfect solution at the outset of the process would create an unnecessary burden.

7 Numerical example

Let us consider the capacitance per unit length for the coaxial system of electrodes, as illustrated in Fig. 8.

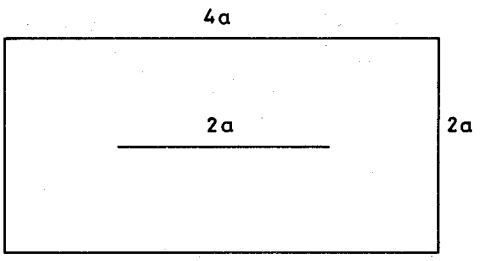

Fig. 8 *Coaxial system of electrodes*

Owing to symmetry only a quarter of the system needs to be investigated. Three different levels of discretisation with decreasing numbers of tubes and slices have been used. The three resultant distributions of subtubes and subslices are shown in Figs. 9, 10 and 11.

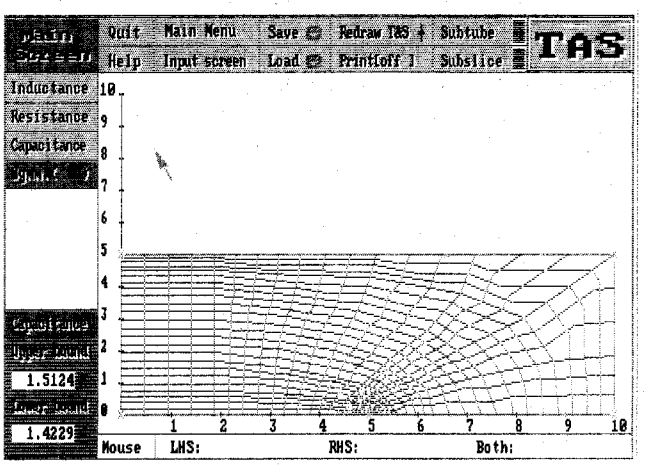

Fig. 9 *Solution for 7 tubes and 6 slices*

It may be instructive to notice that the upper bound of the capacitance, as given by 'rectangular' slices of Fig. 11, can also be found in a simple analytical form:

$$\frac{1}{C} = \frac{1}{\varepsilon_0} \int_0^a \frac{dx}{(a + 2x)}$$

giving $C_+ = 4C = 7.29\,\varepsilon_0$. In general, however, such simple explicit formulas will be difficult to derive, and thus summations described in Section 4 are employed.

Table 1 summarises the results. The capacitance calculated using a finite-element program is also included as a

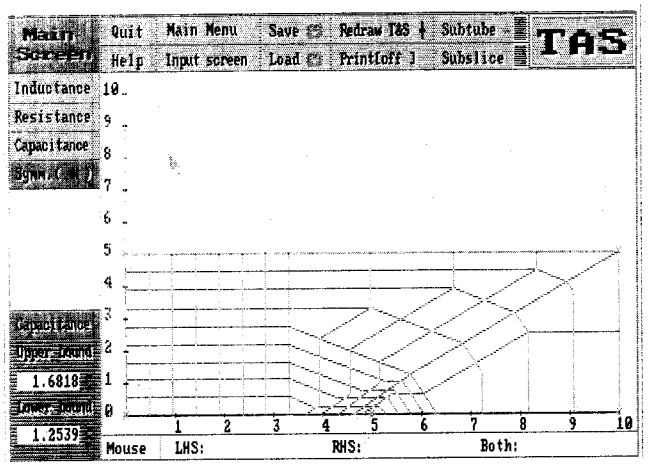

Fig. 10 *Solution for 3 tubes and 2 slices*

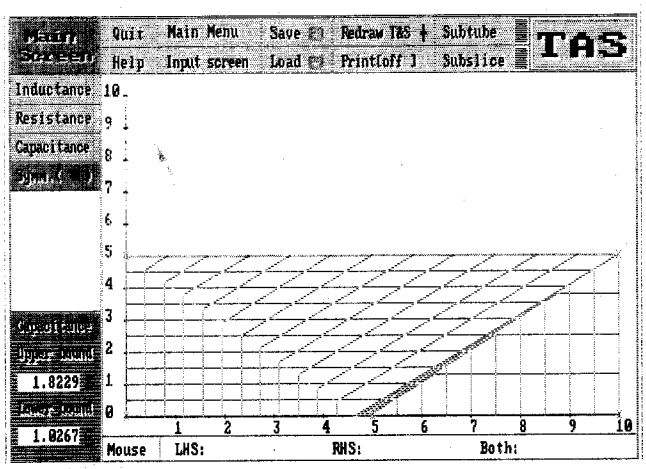

Fig. 11 *Solution for 2 tubes and 1 slice*

Table 1: Capacitance per unit length

Program	All values × ε_0			Error in C_{ave}	Difference in bounds
	Upper bound C_+	Lower bound C_-	$C_{ave} = \frac{C_+ + C_-}{2}$		
TAS 7 tubes × 6 slices	6.05	5.69	5.87	<0.5%	6%
TAS 3 tubes × 2 slices	6.73	5.01	5.87	<0.5%	29%
TAS 2 tubes × 1 slice	7.29	4.11	5.70	2.9%	54%
Finite elements (1600 elements)			5.87		

benchmark value. In particular, the Table shows the effect of decreasing the number of tubes and slices. As might have been expected, the confidence limits given by the two energy bounds deteriorate. What is very encouraging, however, is the fact that the average value remains remarkably stable. Thus, if the global parameter is our ultimate goal, we can safely compromise the local accuracy and still obtain a very accurate final answer.

8 TAS as a teaching aid

Undergraduate courses in electromagnetism typically involve the learning of analytical and numerical methods for attacking electric and magnetic boundary value problems. Very often, the relevance of the modelling concepts to real physical systems and devices is only poorly appreciated. The computational and graphics capabilities of modern personal computers, when supported by appropriate software, provide relatively new opportunities to help students to visualise the behaviour of fields, and therefore to understand difficult concepts. The tubes and slices approach, in general, and the TAS program, in particular, seem to have much to commend them as an educational tool.

Most illustrative examples used in teaching contain a very high degree of symmetry. The use of TAS for this purpose immediately removes such constraints. What is even more important, however, is that this is done under very strict control of the user. For example, a student could easily inquire into how a small departure from a symmetrical system affects the solution.

Secondly, the effects of geometry on field structures have traditionally been expressed in terms of relatively advanced mathematical tools. Too often, the advanced mathematics has tended to obscure rather than promote physical insights. The TAS approach, on the other hand, is physically well based because it uses the inherent properties of the field. Indeed, the whole concept of duality can be based entirely on physical description with little reference to mathematics, although the two formulations are, of course, consistent.

And last but not least, there is an element of active involvement of the user in the TAS computational process, more than supplying the data and looking at the results. The student has to use his knowledge and engineering judgment to initiate the process, and the program responds by providing dual bounds as a feedback signal for further improvements of the solution. This type of truly interactive session puts the student in the role of a designer rather than a passive observer.

9 Conclusions

TAS is the first computer graphics program, for calculating circuit parameters (R, L, C) of distributed systems, based on the dual energy bounds approach known as the method of tubes and slices. The range of applications is still rather restricted, but the program has proved an efficient and low-cost CAD tool.

The method of tubes and slices may be seen as an alternative or complement to other well established methods like finite elements, boundary elements, etc., and is thought to be particularly suitable for teaching purposes.

10 Acknowledgments

The author wishes to thank Mr. M.H. Lam for his valuable contribution during the development of the software. Thanks are also due to Professor P. Hammond and Dr. R.L. Stoll for encouragement and helpful discussions.

11 References

1 HAMMOND, P.: 'Energy methods in electromagnetism' (Clarendon Press, 1981), pp. 63–64
2 HAMMOND, P., ROMERO-FUSTER, M.C., and ROBERTSON, S.A.: 'Fast numerical method for calculation of electric and magnetic fields based on potential-flux duality', *IEE Proc. A*, 1985, **132**, (2), pp. 84–94
3 HAMMOND, P., and ZHAN QIONGHUA: 'Calculation of Poissonian fields by means of the method of tubes and slices', *ibid.*, 1985, **132**, (4), pp. 149–156
4 PENMAN, J., and GRIEVE, M.D.: 'Self-adaptive mesh generation technique for the finite-element method', *ibid.*, 1987, **134**, (8), pp. 634–650
5 PINCHUK, A.M., and SILVESTER, P.P.: 'Error estimation for automatic adaptive finite element mesh generation', *IEEE Trans.*, 1985, **MAG-21**, (6), pp. 2551–2554
6 HAMMOND, P., and TSIBOUKIS, T.D.: 'Dual finite-element calculations for static electric and magnetic fields', *IEE Proc. A*, 1983, **130**, (3), pp. 105–111